Simple fabrication of ultrahigh aspect ratio nanostructures for enhanced antireflectivity

Citation: Dominguez, Sagrario, et al. "Simple Fabrication of Ultrahigh Aspect Ratio Nanostructures for Enhanced Antireflectivity." Journal of Vacuum Science & Technology B, Nanotechnology and Microelectronics: Materials, Processing, Measurement, and Phenomena, vol. 32, no. 3, May 2014, p. 030602. © 2014 American Vacuum Society

As Published: http://dx.doi.org/10.1116/1.4869302

Publisher: American Vacuum Society

Persistent URL: http://hdl.handle.net/1721.1/119017

Version: Final published version: final published article, as it appeared in a journal, conference proceedings, or other formally published context

JVSTB Journal of Vacuum Science & Technology B

Simple fabrication of ultrahigh aspect ratio nanostructures for enhanced antireflectivity

Sagrario Dominguez, Ignacio Cornago, Javier Bravo, Jesus Pérez-Conde, Hyungryul J. Choi, Jeong-Gil Kim, and George Barbastathis

Citation: Journal of Vacuum Science & Technology B **32**, 030602 (2014); doi: 10.1116/1.4869302
View online: http://dx.doi.org/10.1116/1.4869302
View Table of Contents: http://scitation.aip.org/content/avs/journal/jvstb/32/3?ver=pdfcov
Published by the AVS: Science & Technology of Materials, Interfaces, and Processing

Simple fabrication of ultrahigh aspect ratio nanostructures for enhanced antireflectivity

Sagrario Dominguez[a)]
CEMITEC, Noain 31110, Spain and Department of Mechanical Engineering, Massachusetts Institute of Technology, Cambridge, Massachusetts 02319

Ignacio Cornago and Javier Bravo
CEMITEC, Noain 31110, Spain

Jesus Pérez-Conde
Department of Physics, Universidad Pública de Navarra, 31006 Pamplona, Spain

Hyungryul J. Choi and Jeong-Gil Kim
Department of Mechanical Engineering, Massachusetts Institute of Technology, Cambridge, Massachusetts 02319

George Barbastathis
Department of Mechanical Engineering, Massachusetts Institute of Technology, Cambridge, Massachusetts 02319; Singapore-MIT Alliance for Research and Technology (SMART) Center, Singapore 117543; and Shanghai Jiao Tong University–University of Michigan Joint Institute, Shanghai 200240, China

(Received 31 January 2014; accepted 11 March 2014; published 26 March 2014)

In this work, the authors present a novel fabrication process to create periodic nanostructures with aspect ratio as high as 9.6. These nanostructures reduce spectral reflectance of silicon to less than 4% over the broad wavelength region from 200 to 2000 nm. At the visible range of the spectrum, from 200 to 650 nm, reflectivity is reduced to less than 0.1%. The aspect ratio and reflectance performance that the authors achieved have never been reported before for ordered tapered nanostructures, to our knowledge. © *2014 American Vacuum Society*. [http://dx.doi.org/10.1116/1.4869302]

I. INTRODUCTION

Nanostructured surfaces have been widely studied to improve the optical properties of both absorptive and transparent materials, such as Si, GaAs, and fused silica.[1–3] Due to the subwavelength feature size, nanostructures behave as an effective medium with a gradient refractive index, suppressing light reflection at material interfaces through adiabatic impedance matching.[1,2,4–6]

In the case of silicon, many efforts have been undertaken to improve light absorption by texturizing the surfaces. Previous reported solutions achieved reflectance under 1% in the visible wavelength region, but extending these properties to broader bands remained challenging.[7,8] Random distributions of tapered nanostructures are preferred to achieve broadband low reflectance. In fact, most of the black silicon fabrication reported in photovoltaic related literature is based on this kind of structures.[9,10] However, low reflectivity is also achievable using periodic nanostructures, which are more advantageous as they are more controllable, reproducible, and eliminate possibilities for scatter.[11,12]

The geometry of the nanostructures is the key to create surfaces with improved optical properties. To minimize light reflection, it is particularly important to gradually taper the structures with small diameter and large height so as to smoothen the refractive index profile: The higher aspect ratio of nanocone structures (i.e., the ratio of nanocone height to the base diameter) the surface has, the less reflectance it exhibits.[2,13,14] With this purpose, high aspect ratio periodic nanocones have been recently fabricated to increase light transmissivity of glass. Using a multiple shrinking mask etching process, nanocones with an aspect ratio as high as 7 have been successfully fabricated directly on top of a fused silica wafer.[15] Nanoimprint lithography has subsequently been used to replicate these structures in alternate materials to improve their reflectivity.[16,17]

In this work, we present a novel fabrication process based on a single shrinking mask etching step to create periodic nanocones with ultrahigh aspect ratios up to 9.6, in order to achieve ultimate antireflectivity on the surface of silicon in a simpler way compared to the previous works. These nanocones exhibit broadband antireflectivity in the wavelength range between 200 and 2000 nm. Besides, in the visible wavelength range, the reflectance is suppressed almost entirely, to less than 0.1%, thanks to the high aspect ratio. The tapered nature of periodic nanocone arrays makes them suitable for nanoimprint lithography for replication in alternate materials, as in our earlier work,[16,17] broadening the possible applications and promoting the scalability of the technology.[18]

II. EXPERIMENT

The optical behavior of different silicon nanocones has been simulated using the FDTD (i.e., finite-difference time-domain) based software OPTIFDTD. In the simulation model, the diameter of the cone base is fixed to be the same as the period and the top of the cone is reduced to a point. While the period of the structure is set to the minimum value achievable with our fabrication method, 170 nm, three

a)Electronic mail: sdominguez@cemitec.com

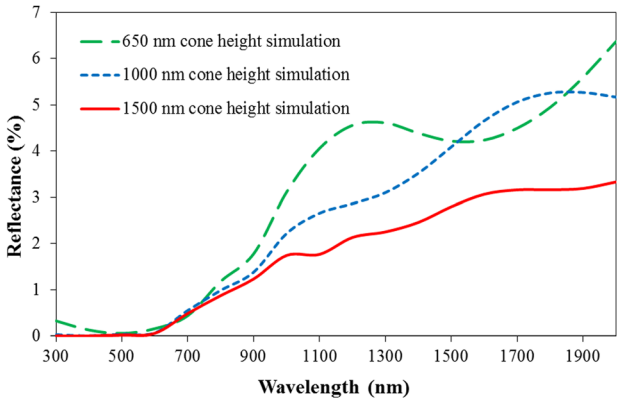

FIG. 1. (Color online) Simulated total reflectance for periodic nanocones with three different heights: 650, 1000, and 1500 nm.

different cone heights are considered. As the height of the cone increases, the change of the effective reflective index between air and silicon becomes smoother and the reflectance occurred at the optical interface decreases, as expected. Figure 1 shows the simulated reflectance for three different heights: 650, 1000, and 1500 nm. The three structures have reflectance lower than 1% between 300 and 800 nm and lower than 7% in the whole studied spectral range from 300 to 2000 nm. Besides, the reflectance is less than 0.1% over the wavelength region from 300 to 600 nm for the nanocones of 1000 nm and 1500 nm height. As expected, minimum reflectance is obtained from the 1500 nm height nanocones, totaling reflected energy of less than 3.5% in the entire simulated range from 300 to 2000 nm.

The height of the nanocone should be chosen according to the desired application. In the case of the photovoltaic field, very high aspect ratio structures are not necessarily required as they can negatively affect the charges collection and recombination.[19,20] Besides, as the silicon band gap is at 1150 nm, it is not necessary to reduce reflectance for higher wavelengths. Therefore, the silicon nanocones of 650 nm or 1000 nm height could be enough for solar cell applications. However, higher aspect ratio is still desirable for applications with more broadband antireflection requirements, such as wide-band detector or microwave absorber.[21,22]

The fabrication process for ultrahigh aspect ratio nanocone arrays is shown in Fig. 2. First, a trilayer for interference lithography is deposited on top of a silicon wafer: an antireflective coating (ARC, XHRiC-16, Brewer Science, Inc.) to minimize the reflection of light during laser exposure, a thin SiO_2 layer for improving the pattern transfer to the ARC, and a negative photoresist layer (THMR-iN PS4 MG, TOKYO OHKA KOGYO CO., LTD) where the pattern is initially recorded. Then, the sample is illuminated with a laser light source at 325 nm wavelength by using a Lloyd's Mirror interferometer lithographic setup, and after that, the exposed photoresist is developed to obtain a periodic array of holes (Fig. 2.1). In the second step (Fig. 2.2), this pattern is transferred to the SiO_2 interlayer and subsequently to the ARC with CF_4 and O_2 reactive ion etching (RIE), respectively. Subsequently, hydrogen silsesquioxane (HSQ14, Dow Corning) is spun on the ARC holes and baked at 200 °C (Fig. 2.3). Part of this layer fills the ARC holes, while the rest remains on top surface of ARC. The HSQ excess layer on top of the ARC is first removed by CF_4 RIE (Fig. 2.4), and then, the remaining ARC is removed by O_2 RIE obtaining a pattern of HSQ posts over the silicon (Fig. 2.5). This pattern is used as a shrinking mask to create the silicon nanocones during HBr RIE (Fig. 2.6). HSQ posts are a good mask since the HSQ etch rate is slower than that of Si

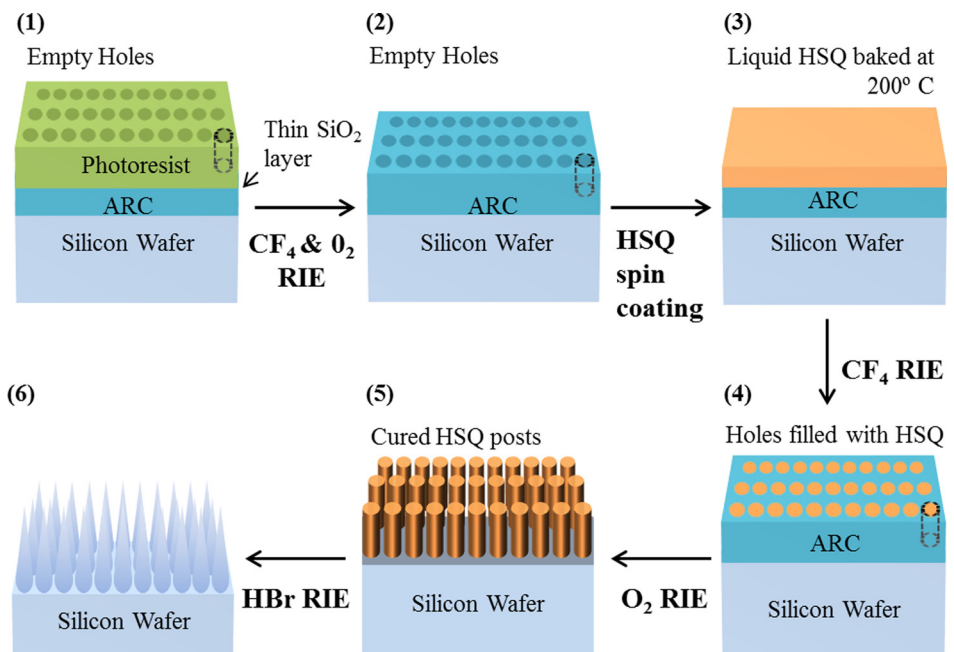

FIG. 2. (Color online) Fabrication process followed to fabricate nanocones with aspect ratios as high as 9.6. The process is based in laser interference lithography (LIL) and RIE.

in HBr plasma, and it also shrinks laterally while Si is etched deeper, enabling conical shaping of the nanostructures.

Depending on the HSQ mask dimensions and HBr RIE conditions, different aspect ratio nanocones can be fabricated. To obtain high aspect ratio, the dimensions of the HSQ posts have to be large enough to resist a deep-transfer process. To maximize the diameter, we use a negative photoresist and the HSQ image reverse process explained before due to the limitation on feature sizes of positive photoresists.[15] The HSQ posts height is limited by the ARC thickness used in the interference lithography process.

Etching conditions have to be optimized to obtain the optimal shrinking speed of the HSQ mask, to reach the desired structure. 9.6 aspect ratio nanocones with a period of 170 nm and a height of 1640 nm have been fabricated during 25 min of 20 sccm HBr etching process with a chamber pressure of 20 mTorr and a power of 150 W.

III. RESULTS AND DISCUSSION

Cross-sectional scanning electron micrographs of three different patterns of HSQ posts on silicon substrates are shown in Figs. 3(a)–3(c). The nanocones obtained by using each of these patterns as the mask during the HBr RIE are shown in Figs. 3(d)–3(f). All the structures have a period of 170 nm, which is the minimum value achievable with laser interferometer lithography at 325 nm of wavelength. Starting with a 100 nm height HSQ posts mask, nanocones of 650 nm height are created. When the mask height is increased to 140 and 200 nm, the height of nanocones can be increased up to 1000 nm and 1640 nm, respectively. In all cases, the cones were fabricated so as to have a linear graded profile, because the etch rates of HSQ posts and silicon during RIE process were optimized to be constant. The diameter of the structures ranges from 170 nm at the bottom, where adjacent cones are touching each other, to less than 20 nm at the sharp tip at the top. Thus, we achieve a gradual and slow variation of the effective refractive index from the index of air on the tip of the cone to the index of silicon on the base.

Reflectance measurements of the nanostructured surface with 1640 nm height nanocones over a wavelength range from 200 to 2000 nm are presented in Fig. 4. A spectrophotometer (JASCO V-670) with an integrating sphere (JASCO ISN-723) was used to measure the total reflectance which is the sum of the specular and the diffuse components. Specular reflectance corresponds to the light coming back from the surface at the normal direction of the surface (0°), and it is under 4% between 200 and 2000 nm. This means a drastic reduction of silicon reflectance, whose general value is around 30% in the same spectral range with polished surface.

To separate specular from diffuse reflectance, we tilted the sample by a small angle relative to the tangential orientation with respect to the integrating sphere's entrance aperture. Thus, the light is normally incident so specular reflection goes backward toward the source and is rejected by the sphere. Due to the tilt of the sample, a small part of the diffuse light misses the entrance to the integrating sphere, while most of it finds its way in. Since the tilt required for the sample in our apparatus is small (~5°), the solid angle subtended that misses the integrating sphere's entrance is approximately 1% of 4π. Further, assuming the diffuse light to be quasi-isotropically distributed, the same estimate of 1% should correspond to the loss of diffuse light in our approach.

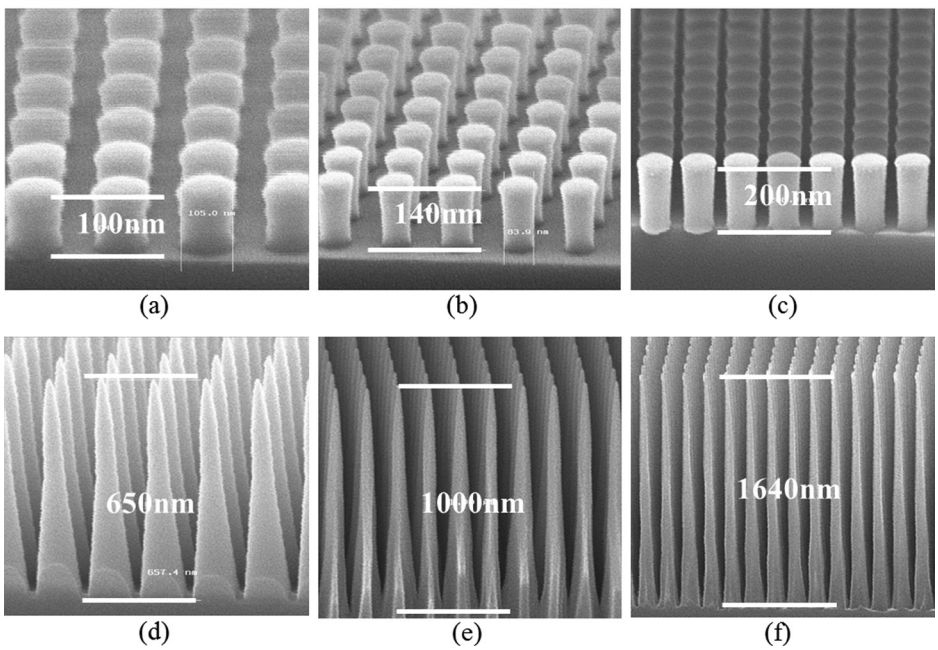

FIG. 3. Cross-sectional scanning electron micrographs of three HSQ posts masks used in the HBr RIE process and of the three different final nanocone patterns. Three different heights of HSQ posts have been used: (a) 100 nm, (b) 140 nm, and (c) 200 nm and three different heights have been obtained: (d) 650 nm, (e) 1000 nm and (f) 1640 nm, respectively. All nanostructures have a period of 170 nm.

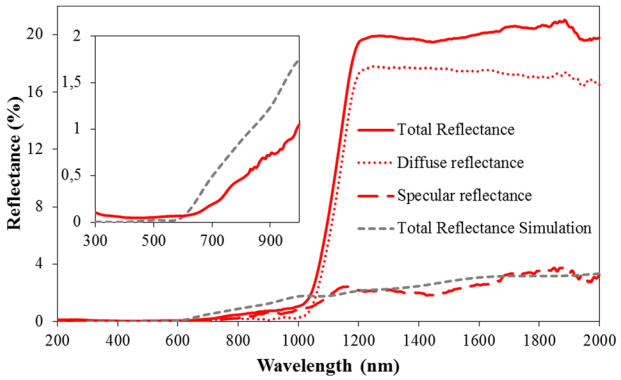

FIG. 4. (Color online) Summed specular and diffuse reflectance measurements for periodic patterns of 9.6 aspect ratio nanocones with a period of 170 nm and a height of 1640 nm. Simulation results of the total front-side reflectance are also shown for comparison. In the left inset, a more detailed graph for both the measurements and the simulation of the total reflectance between 300 and 1000 nm is shown.

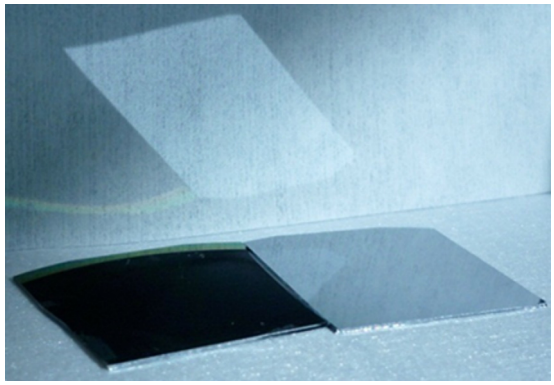

FIG. 5. (Color online) Comparison between samples of silicon patterned with a periodic array of cones with a period of 170 nm and a height of 1640 nm (aspect ratio of 9.6) on the left and an untreated polished crystalline silicon on the right. At the back, the reflected image of the samples can also be observed when the sample is illuminated by sunlight.

With these caveats, the result of the integrating sphere measurement for diffuse reflectance (i.e., light backscattered at all angles from $-90°$ to $90°$ except the specular reflection direction) is less than 0.5% at wavelengths from 200 nm to 1050 nm, where it abruptly increases to approximately 18%.This steplike behavior of the curve is due to nonabsorbed light reflecting on the backside of the silicon wafer. For wavelengths higher than 1050 nm, light is not absorbed in the silicon, so it goes through the wafer reflecting again at the optical interface between the backside of the silicon wafer and the air.[23,24] The silicon wafers used for sample fabrication are single side polished, and they have a rough back surface. The light reflected from the back is diffused so that there is no abrupt rise around 1050 nm of wavelength in the specular reflectance measurements. If the goal is to have broadband antireflection, nanocones could be patterned at both sides of the wafer to let the light pass through the substrate.[6] Total reflectance corresponds to the light coming back at any angle, and it is the sum of both the specular and the diffuse components. Therefore, it also exhibits the same sharp rise at around 1050 nm due to diffuse backside reflection. Simulation data of the total reflectance are also shown in Fig. 4 for comparison. In the simulation, only the reflectance from the front surface was considered, so as to avoid the diffuse backside reflection effect. Therefore, the simulation is only comparable with the experimental total reflectance until 1050 nm. In the left inset of Fig. 4, both curves are shown in detail between 300 and 1000 nm. Reflectance is under 1% in that region being depicted and under 0.2% between 300 and 700 nm. The slight differences between simulation and measurements in this wavelength range could be due to the defects introduced in the fabrication process that are not considered in the simulation model. For longer wavelengths, the good agreement between the simulation and the specular measurements give us confidence that the diffuse component coming from the front surface is very low and the total reflectance from the front surface is also less than 4% until 2000 nm. This is one of the best antireflection results for silicon in the literature, to our knowledge.

The almost complete suppression of reflectivity in the range of visible wavelengths leads to the black appearance of the silicon sample shown in Fig. 5. A piece of the sample with 1640 nm height nanocones, in the left, is shown together with a flat silicon surface, in the right, for comparison. In the back of the image, the reflection of the samples illuminated by sunlight can also be observed. While there is a bright reflection coming from the polished surface, no reflection can be seen from the nanocone-patterned silicon.

IV. SUMMARY AND CONCLUSIONS

As a conclusion, periodic nanocone patterns have been fabricated following a simple method which allows to create slender nanostructures with aspect ratios as high as 9.6. These nanocones drastically reduce reflectance to values under 4% in the broadband wavelength range between 200 and 2000 nm and under 0.2% in the visible range of light. Both the aspect ratio and the reflectance results have never before been reported for ordered structures, to our knowledge. The fabricated high aspect ratio nanocone arrays are superior in terms of antireflectivity, and the simple fabrication process implemented here is promising for applications such as photovoltaic cells and wide-band sensors or absorbers.

ACKNOWLEDGMENTS

The authors would like to thank the staff and facility support from the Nano Structures Laboratory at MIT, especially T. A. Savas for his continuous help during the processing and for contributions in the HSQ masking process, and J. Daley for all his help in the lab. This work was supported in part by Department of Innovation, Enterprise and Employment of Gobierno de Navarra research Grant 1858/2012, by the MIT Institute for Soldier Nanotechnologies (ISN) under Contract DAAD-19-02D-0002 with the U.S. Army Research Office, and by the Singapore National Research Foundation (NRF) through the Singapore-MIT Alliance for Research and Technology (SMART) Centre.

[1]J. Zhao, A. Wang, M. A. Green, and F. Ferrazza, Appl. Phys. Lett. **73**, 1991 (1998).

[2]K.-C. Park, H. J. Choi, C.-H. Chang, R. E. Cohen, G. H. McKinley, and G. Barbastathis, ACS Nano. **6**, 3789 (2012).
[3]P. L. Gourley, J. R. Wendt, G. A. Vawter, T. M. Brennan, and B. E. Hammons, Appl. Phys. Lett. **64**, 687 (1994).
[4]S. Domínguez, I. Cornago, O. García, M. Ezquer, M. J. Rodríguez, A. R. Lagunas, J. Pérez-Conde, and J. Bravo, Photonics Nanostruct. **11**, 29 (2013).
[5]S. Domínguez, O. García, M. Ezquer, M. J. Rodríguez, A. R. Lagunas, J. Pérez-Conde, and J. Bravo, Photonics Nanostruct. **10**, 46 (2012).
[6]I. Cornago, H. J. Choi, J.-G. Kim, and G. Barbastathis, 38th International Conference on Micro and Nano Engineering, Toulouse, France, 16–20 September 2012.
[7]S. Chattopadhyay, Y. F. Huang, Y. J. Jen, A. Ganguly, K. H. Chen, and L. C. Chen, Mater. Sci. Eng., R **69**, 1 (2010).
[8]L. L. Ma, Y. C. Zhou, N. Jiang, X. Lu, J. Shao, W. Lu, J. Ge, X. M. Ding, and X. Y. Hou, Appl. Phys. Lett. **88**, 171907 (2006).
[9]H. M. Branz, V. E. Yost, S. Ward, K. M. Jones, B. To, and P. Stradins, Appl. Phys. Lett. **94**, 231121 (2009).
[10]S. H. Tan, C. B. Soh, W. Wang, S.-J. Chua, and D. Chi, Appl. Phys. Lett. **101**, 133906 (2012).
[11]K. N. Nguyen, D. Abi-Saab, P. Basset, E. Richalot, F. Marty, D. Angelescu, Y. Leprince-Wang, and T. Bourouina, Microsyst. Technol. **18**, 1807 (2012).
[12]Y. Liu and M. Hong, J. Mater. Sci. **47**, 1594 (2012).
[13]F. Llopis and I. Tobias, J. Appl. Phys. **100**, 124504 (2006).
[14]Y. Li, J. Zhang, and B. Yang, *9th IEEE Conference on Nanotechnology, 2009, IEEE-NANO 2009*, 26–30 July 2009, pp. 1–3.
[15]H. J. Choi, I. Cornago, J.-G. Kim, T. Savas, and G. Barbastathis, *2012 International Conference on Optical MEMS and Nanophotonics (OMN)*, 6–9 Aug. 2012, pp. 1–2.
[16]J.-G. Kim, H. J. Choi, H. Gao, I. Cornago, C.-H. Chang, and G. Barbastathis, *2012 International Conference on Optical MEMS and Nanophotonics (OMN)*, 6–9 Aug. 2012, pp. 71–72.
[17]H. Hauser, B. Michl, S. Schwarzkopf, V. Kübler, C. Müller, M. Hermle, and B. Bläsi, IEEE J. Photovolt. **2**, 114 (2012).
[18]A. A. Letailleur, K. Nomenyo, S. M. Murtry, E. Barthel, E. Søndergård, and G. Lérondel, J. Appl. Phys. **109**, 016104 (2011).
[19]K. Xiong, S. Lu, D. Jiang, J. Dong, and H. Yang, Appl. Phys. Lett. **96**, 193107 (2010).
[20]J. Oh, H.-C. Yuan, and H. M. Branz, Nat. Nanotechnol. **7**, 743 (2012).
[21]D. Rossberg, Sens. Actuators, A **47**, 413 (1995).
[22]X. Liu, Z. Zhang, and Y. Wu, Composites, Part B **42**, 326 (2011).
[23]Y. Kanamori, M. Sasaki, and K. Hane, Opt. Lett. **24**, 1422 (1999).
[24]M.-L. Kuo, D. J. Poxson, Y. S. Kim, F. W. Mont, J. K. Kim, E. F. Schubert, and S.-Y. Lin, Opt. Lett. **33**, 2527 (2008).